A Model for Parison Behavior in the Extrusion Blow Molding Process

A simple, lumped-parameter model has been developed to predict the length and shape of a parison on the basis of experimental swell data and the storage modulus of the resin. The applicability and limitations of the model are demonstrated by comparing its predictions with experimental observations of parison behavior.

J. M. DEALY and
NESE ORBEY
Department of Chemical Engineering,
McGill University
Montreal, Canada H3A 2A7

SCOPE

In the extrusion blow molding process for manufacturing plastic bottles and other hollow articles, the first step in the molding cycle is the extrusion, vertically downward, of a tube or "parison" of molten plastic. The parison is then inflated to take the shape of a mold that has been closed around it. The shape and thickness distribution of the finished container depend on the dimensions of the parison at the time of inflation. The geometry of the parison is, in turn, governed by the deformation of the molten polymer after it exits the die. In particular, the processes of swell and sag act to cause a variation of parison dimensions between the time the melt emerges from the die and the moment of inflation. Many attempts have been made to correlate parison behavior to rheological properties that can be measured in the laboratory, but there has been little success to date. The aim of the present study was to develop a simple model to predict parison shape using only a few parameters that can be determined in the laboratory and not requiring extensive computation. The model predictions were compared with experimental data obtained using different die geometries, extrusion rates, and parison weights.

CONCLUSIONS AND SIGNIFICANCE

A simple model has been developed to predict the shape of the parison at the moment of inflation. The model is intended to provide a basis for resin selection, equipment design, and process control. Its use requires extrudate swell and storage modulus data, which can be obtained in the laboratory, and the equations can be solved using a personal computer. The model is found to predict parison length with acceptable accuracy except at high extrusion rates and in the case of a diverging die, for which the diameter swell is very large.

INTRODUCTION

In extrusion blow molding, the shape of the extruded tube of molten plastic—the parison—and its thickness distribution at the moment the mold closes are of central importance. If there are handles or tabs on the molded object or if it is otherwise unsymmetrical, control of parison shape is essential if an acceptable product is to be produced. The thickness distribution of the parison has a direct influence on that of the molded object, and here the objective is to provide adequate strength with the minimum use of resin.

It is highly desirable to be able to predict parison behavior on the basis of laboratory measurements of melt properties, and the goal of the work reported here was to develop a simple model that could be used for such a prediction. In order to avoid elaborate computations, it has been customary to simplify the problem by considering parison formation to be the result of two phenomena, swell and sag (or "draw-down").

In recent years, several semiempirical models have been proposed to predict parison behavior in which both sag and swell were considered (Cogswell et al., 1971; Henze and Wu, 1973; Ajroldi, 1978; Kamal et al., 1981; Dutta and Ryan 1982). However, these models require parameters that are not easy to obtain and there is not enough experimental evidence to validate them.

The goal of the present approach was to develop a model that requires only a few resin properties that can be obtained using commercially available or easily constructed laboratory equipment, and which is mathematically simple enough so that the calculations can be carried out on a personal computer.

For a blow molding die, two swell ratios are required to describe the relationship between the parison cross section and that of the die at its exit. While there are several ways of defining swell ratios, we have chosen to use a diameter swell (B_1) and a thickness swell (B_2), defined as $B_1 \equiv D_p/D_o$, and $B_2 \equiv h_p/h_o$, where D_p and D_o are the outside diameters of the parison and the die lips respectively, and h_p and h_o are the parison thickness and die gap respectively, as shown in Figure 1.

Correspondence concerning this paper should be directed to J. M. Dealy.
Nese Orbey is with the Department of Chemical Engineering, Middle East Technical University, Ankara, Turkey.

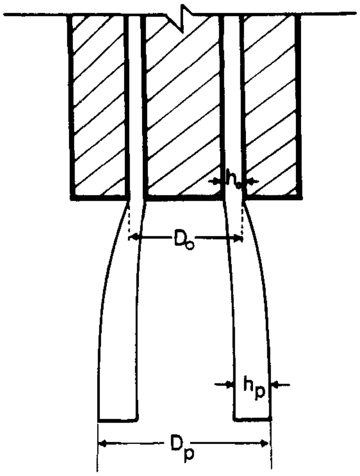

Figure 1. Symbols used to define swell ratios.

Many attempts have been made to relate extrudate swell to rheological properties, but none of these approaches has led to a reliable predictive method valid at high flow rates. For the present, then, it is not possible to incorporate into a parison model a reliable method for predicting swell. Thus, the model described here predicts parison geometry starting from measured swell values together with a rheological analysis of the sag process.

EXPERIMENTAL PROCEDURES

A blow-molding-grade high density polyethylene resin was used in the experiments. The resin (McGill stock No. 27), Union Carbide Canada DMDJ-5140, has a melt index of 0.96 with $\overline{M}_w = 1.25 \times 10^5$ and $\overline{M}_n = 1.76 \times 10^4$. Rheological properties of this resin (viscosity and first normal stress difference as functions of shear rate, storage modulus, and complex viscosity as functions of frequency) have been reported elsewhere (Orbey, 1983; Orbey and Dealy, 1984). Three annular die geometries were used: a straight die, a 20° diverging die, and a 20° converging die. The major features of the flow geometry of these dies are shown in Figure 2. In all cases the annular gap at the die lips was 1.5875 mm and the total length was 69.85 mm. These dies are described in detail elsewhere (Orbey, 1983; Orbey and Dealy, 1984).

Two types of experiments were carried out. In the first set, parison swell was studied in the absence of gravitational forces. In the second set, the combined effects of sag and swell were studied and the model predictions were compared with these data. All experiments were carried out at 170°C under isothermal conditions.

Pure swell data in the absence of sag were obtained by extruding the parison directly into an oil bath that was at the same temperature as the extrudate and had a density carefully matched to that of the melt. In this way sag was completely eliminated. Diameter and thickness swell values were obtained photographically as functions of time. The experimental apparatus and technique used in these experiments together with the results obtained are presented elsewhere (Orbey and Dealy, 1984; Orbey 1983). The reproducibility of the swell vs. time data was determined by carrying out six experiments under identical conditions. The standard deviation was found to be less than 0.02 at all times.

It was found that 60–80% of the swell occurs in the first few seconds after the parison leaves the die, with an equilibrium value being reached after 5–8 minutes have elapsed. The thickness swell values from the three die geometries were found to be quite similar, but the diameter swell at a given flow rate increased substantially as the die shape was altered in the following

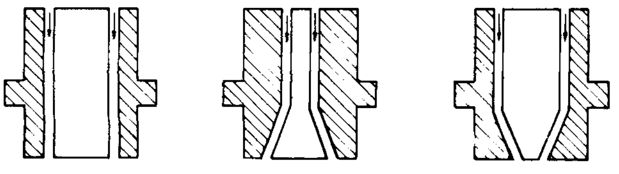

Figure 2. Cross sections of the dies.

TABLE 1. PARAMETERS OF EQ. 1 FOR DIAMETER SWELL (RESIN 27)

Q(cm^3/s)	B_o	B_∞	ζ(1/s)
Straight Die			
0.095	1.25	1.66	132
0.238	1.29	1.70	109
0.475	1.33	1.74	57
0.950	1.35	1.76	69
2.375	1.38	1.94	103
Diverging Die			
0.475	1.02	1.31	160
0.950	1.05	1.38	162
20° Converging Die			
0.475	1.92	2.81	110
0.950	2.10	2.70	45

TABLE 2. PARAMETERS OF EQ. 1 FOR THICKNESS SWELL (RESIN 27)

Q(cm^3/s)	B_o	B_∞	ζ(1/s)
Straight Die			
0.095	1.17	1.84	268
0.238	1.24	1.86	218
0.475	1.43	1.92	211
0.950	1.48	1.97	129
2.375	1.56	2.10	154
Diverging Die			
0.475	1.40	1.97	150
0.950	1.47	2.15	185
20° Converging Die			
0.475	1.29	1.92	143
0.950	1.31	1.81	55

order: diverging, straight, converging. The experimental swell data were fitted to an equation proposed by Garcia-Rejon and Dealy (1982), which was found to give a good fit of the data for both thickness and diameter swells:

$$B(t) = B_0 + (B_\infty - B_o)(1 - e^{-t/\zeta}) \quad (1)$$

The values of the constants for the resin used in this study are given in Tables 1 and 2.

The combined effect of sag and swell was studied by extruding the parison into an isothermal air oven instead of an oil bath. An Instron capillary rheometer was used to extrude the polymer at different crosshead speeds. The air oven had a front window which permitted observation of the parison. Photographs of the parison were taken during the extrusion and post-extrusion stages, and the length of the parison was monitored as a function of time.

DESCRIPTION OF THE MODEL

In the present model, the parison is considered to be made up of a number of cylindrical elements of finite length L_i, each having the same mass, that being the amount of resin extruded in a fixed time interval, Δt. This is shown schematically in Figure 3. This approach of considering the parison to be made up of individual elements allows us to model parison behavior without recourse to numerical analysis. The time interval Δt is chosen to be an integral fraction of the total extrusion time t_e, so that at the end of extrusion the number of elements will be an exact integer. Element no. 1 is the first one extruded, while at any instant of time t, N denotes the last complete element to be extruded. Thus, N is the next integer below $t/\Delta t$. The element currently being extruded corresponds to $i = N + 1$.

The analysis is carried out in two stages. First, the element that is currently being extruded is considered. The length of the element currently being extruded increases by an amount dL during a time interval dt. Taking the density to be constant, dL is related to the average melt velocity at the die exit v_d, the area of the die exit A_d, and the area of the parison element $A_i(t)$, as follows:

$$dL_{N+1} = \frac{A_d v_d dt}{A_i(t)} \quad (2)$$

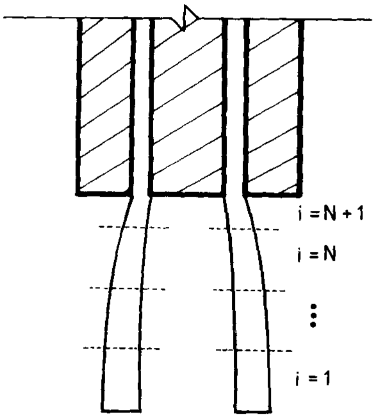

Figure 3. Schematic diagram of parison elements.

The element formation time Δt is sufficiently small that we can neglect the sag that occurs during this period. Then $A_i(t)$ depends only on swell, and if the parison thickness is small compared to its radius, the ratio $A_i(t)/A_d$ can be approximated as the product of the two swell ratios. Using this approximation and integrating:

$$L_{N+1}(t) = \int_{N\Delta t}^{t} \frac{v_d dt'}{B_1(t')B_2(t')} \tag{3}$$

Equation 1 was used to represent the functions $B_1(t)$ and $B_2(t)$ in the model. Noting that nearly 70% of the swell occurs very quickly, with the remainder taking place much more gradually, the integral in Eq. 3 can be simplified by using approximate average values of the swell ratios.

$$L_{N+1}(t) = \frac{v_d(t - N\Delta t)}{B_1(\Delta t/2)B_2(\Delta t/2)} \tag{4}$$

To find the length of an element that is fully formed, both sag and swell have to be considered. If t_i is the time that has elapsed since element i was fully extruded, and t is the total time since parison extrusion commenced:

$$t_i = t - i\Delta t \tag{5}$$

It is assumed that the sag of an element occurs independently of swell and that sag can be modeled in terms of the uniaxial extension of a hypothetical unswollen element. To this end, Z_i is defined to be the hypothetical length that element i would have if there had been no swell. The Hencky strain rate, ϵ_i, of the element is given by:

$$\epsilon_i(t_i) = \frac{1}{Z_i}\frac{dZ_i}{dt_i} \tag{6}$$

Since sag is neglected during the formation of the element, at time $t_i = 0$

$$z_i(0) = v_d \Delta t \tag{7}$$

To evaluate $Z_i(t_i)$, the Hencky strain rate must be related to the net stretching stress by a rheological constitutive equation for the melt. The net stretching stress is the weight of the $(i - 1)$ elements below, divided by the hypothetical area A_i' of the unswollen element:

$$\tau_{zz} - \tau_{rr} \equiv \tau_i = \frac{(\rho v_d A_d \Delta t)(i - 1)g}{A_i'} \tag{8}$$

From continuity, with the density assumed constant:

$$Z_i A_i' = v_d A_d \Delta t \tag{9}$$

Thus

$$\tau_i = \rho g (i - 1) Z_i \tag{10}$$

To complete the system of equations for calculating $Z_i(t_i)$, a constitutive equation must be selected. For this application, the Lodge "rubberlike liquid" model with three relaxation times was used. The reason for this selection is explained in the next section.

Applying this model to the present case where the parison elements are subjected to a time-dependent strain rate, $\epsilon_i(t_i)$, for $t_i \geq 0$, the following equation for the stress is obtained:

$$\tau_i = \left(\sum_k G_{ok} e^{-t_i/\lambda_{ok}}\right)\left(\frac{Z_i^2(t_i)}{Z_i^2(0)} - \frac{Z_i(0)}{Z_i(t_i)}\right) - \int_0^{t_i}\left(\sum_k \frac{G_{ok}}{\lambda_{ok}} e^{-(t_i - t')/\lambda_{ok}}\right)\left(\frac{Z_i(t')}{Z_i(t_i)} - \frac{Z_i^2(t_i)}{Z_i^2(t')}\right)dt' \tag{11}$$

where G_{ok} is the relaxation modulus corresponding to a relaxation time of λ_{ok}, and $Z_i(0)$, $Z_i(t_i)$, $Z_i(t_i')$ are the values of Z_i at time zero, at time t_i, and at a past time t_i', respectively.

The actual length of an element at any time after it has been fully formed can be obtained by taking account of the swell as follows:

$$L_i(t_i) = \frac{Z_i(t_i)}{B_1(t_i + \Delta t/2)B_2(t_i + \Delta t/2)} \tag{12}$$

Again, Eq. 1 was used to represent the swell functions. The total length of the parison at any time t is obtained by summing up the individual contributions of each element.

$$L(t) = \frac{v_d(t - N\Delta t)}{B_1(\Delta t/2)B_2(\Delta t/2)} + \sum_{i=1}^{N} L_i(t_i) \tag{13}$$

Note that once the parison is fully formed $(t \geq t_e)$ the first term on the righthand side disappears.

The experimental data indicated that zero parison length corresponds to a time which is larger than zero. This phenomenon, which is not uncommon in intermittent extrusion, is due to the compression of the melt in the extruder as pressure builds up prior to flow. This causes a time lag, t_c, so that the real extrusion time is less than the calculated one. In this case the $L(t)$ term in Eq. 13 is replaced by $L(t^*)$ where t^* is defined as follows:

$$t^* = t + t_c \tag{14}$$

The value of t_c can be obtained by extrapolating experimental $L(t)$ data to $L = 0$.

The model performance was evaluated in terms of the length of the parison, since this is the most easily measured quantity. However, the model can be extended to approximate the distributions of diameter and thickness swell in the parison. The area of an element can be calculated from a material balance, and it is assumed that the quotient of swell ratios for the parison is equal to that for the parison extruded into oil:

$$A_i = v_d A_d \Delta t / L_i(t_i) \tag{15}$$

$$\frac{B_{1i}}{B_{2i}} = \frac{B_1(t_i)}{B_2(t_i)} \tag{16}$$

The model does not take account of the atypical nature of the portion of the parison extruded at the beginning of each cycle in the actual blow molding operation. The resin that forms the bottom tip of the parison has been sitting at rest and relaxing near the die lips for several seconds prior to being extruded and thus experiences less shearing and exhibits less swell than the resin making up the remainder of the parison. However, this portion represents only a small fraction of the parison length, and it is mainly incorporated into the discarded tail flash rather than the wall of the finished container.

SELECTION OF A CONSTITUTIVE EQUATION

The length of the parison, in a situation where sag is significant, is the resultant of the competitive influences of sag and swell. This is illustrated in Figure 4, in which are sketched hypothetical length vs. time curves for fully-formed parisons corresponding to three cases. When there is no sag, the parison simply recoils to a steady state length due to swell, as shown by curve 1. If there is sag but no swell, the parison simply elongates due to its own weight until ductile failure occurs near the die. In the actual case, there is often a period over which there is a balance between sag and swell so that the parison length goes through a minimum, as shown by curve 3.

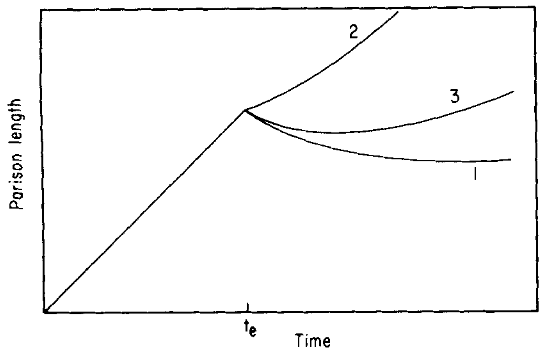

Figure 4. Parison behavior under different conditions: (1) no sag; (2) no swell; (3) actual case.

In our experiments, this minimum was often rather broad, making it appear that the parison was in an equilibrium state. However, from a rheological point of view, this is very much a dynamic situation, and it was found that the shape of the predicted $L(t)$ curve is very sensitive to the constitutive equation used to model the sag process. Since one of our objectives was to avoid any unnecessary complexity in the model, we sought the simplest equation that is capable of describing small departures from linear viscoelasticity in uniaxial extension. The nonlinear effects were expected to be fairly mild because the strain rate and total strain involved are both relatively small. On the other hand, it was found that the assumption of linear viscoelastic behavior always leads to highly inaccurate predictions of parison length.

In some of the previous work on the modeling of parison behavior it has been suggested that the use of a constitutive equation might be avoided altogether by assuming a direct relationship between sag and various experimentally determined material functions, including the extensional creep compliance (Ajroldi, 1978; Kamal et al., 1981) and the extensional stress growth function (Garcia-Rejon et al., 1981). However, such an approach ignores the detailed role played by the strain history, and we found it to be unrealistic and unreliable.

For the present application, it was found that the Lodge "rubberlike liquid" model with three relaxation times gives satisfactory agreement with experiment. This equation, also known as the "convected Maxwell model," is known to give good predictions of transient elongational flows at low extension rates or short times (Lodge, 1974; Bird et al., 1977). The relaxation moduli corresponding to three discrete relaxation times were determined from the linear spectrum and are given in Table 3. The spectrum was, in turn, determined from experimental storage modulus data using Tschoegl's (1971, 1973) second approximation formula.

Calculation Procedure

To obtain the value of $Z_i(t_i)$, Eqs. 10 and 11 were solved simultaneously using a trial and error procedure. Equation 11 is integrated numerically, since the function $Z_i(t_i)$ is not known *a priori*. A composite integration formula was used whereby the integration interval $(t_i - 0)$ was subdivided into smaller intervals of $\Delta\theta$ and the trapezium rule was applied to each small interval (Carnahan et al., 1969). The small time interval for integration, $\Delta\theta$, was taken to be an integer fraction of Δt for convenience. Since Eq. 12 requires knowledge of the value of $Z_i(t_i)$ at past times, it is best to start the calculation with t^* equal to $(t_c + \Delta\theta)$ and increase in time in increments of $\Delta\theta$.

A small computer (PET Commodore 2001) was used to solve the model equations (Orbey, 1983).

TABLE 3. RELAXATION TIMES AND MODULI

λ_{ok}(s)	G_{ok}(Pa)
0.316	16,956
3.160	6,357
31.600	1,420

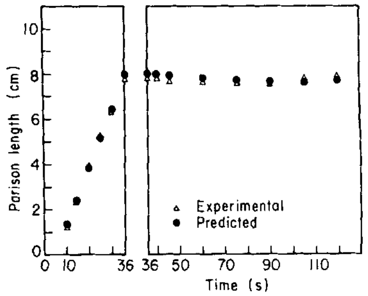

Figure 5. Comparison of experimental and predicted values of parison length. Straight die, m = 6.8 g, Q = 0.238 cm³/s.

COMPARISON OF PREDICTIONS WITH EXPERIMENTAL DATA

The model predictions were compared with experimental data for different die geometries, parison weights, and extrusion rates, and the results are shown in Figures 5–10. The data are presented in two parts because different time scales are used in the extrusion and post-extrusion stages. The first section represents the extrusion stage. The second section starts with the end of extrusion and continues into the post-extrusion stage. At long times in the post-extrusion stage the parison starts necking at the tip of the die and eventually collapses under its own weight. The experimental results showed that once the parison starts necking, the reproducibility of the data becomes very poor. Therefore, the length vs. time data are presented only up to the onset of necking. As can be seen, data were taken for rather long periods after extrusion had been halted. In the blow molding process inflation occurs immediately following extrusion so that this post-extrusion period does not appear to correspond to a stage of the actual process. However, in the production of large containers, very long parisons are formed and significant sag occurs during the extrusion stage. Since our experimental parisons were rather short, significant sag effects could only be studied by extending observations to long post-extrusion times.

Figures 5–8 show both the experimental and the predicted parison lengths for the straight die. Results are presented for two parison weights and three extrusion velocities. The experimental data and model predictions are found to be in good agreement, especially in the extrusion stage and at short times in the post-extrusion stage, which are the important time periods in a commercial blow molding process. At longer times in the post-extrusion stage, the model predictions are higher than the experimental data, especially at the highest extrusion rate (see Figure 8). We believe that this reflects the substantial shear thinning that occurs in the die gap at large shear rates. It is now recognized (Dealy and Tsang, 1981) that the "disentanglement" that accompanies shearing at high strain rates continues to affect the rheological behavior of a melt for a long period of time. This could be accounted for through the use of a structure-dependent relaxation spectrum. To test this idea, the model developed by Acierno et al. (1976) was used. This model has the distinctive feature of having relaxation times and moduli that depend upon the existing structure, i.e., the strain history. However, the use of a structure-dependent relaxation spectrum did not improve the prediction of parison length.

The performance of the model for the diverging die is shown in Figure 9. As in the case of the straight die, the model predictions

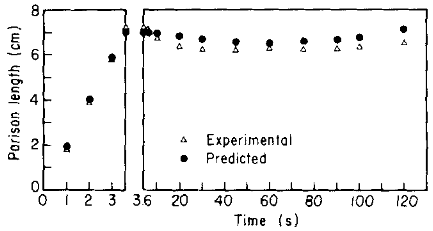

Figure 6. Comparison of experimental and predicted values of parison length. Straight die, m = 6.8 g, Q = 2.375 cm³/s.

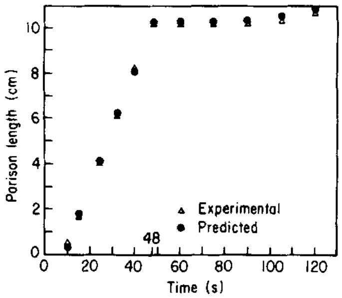

Figure 7. Comparison of experimental and predicted values of parison length. Straight die, m = 9 g, Q = 0.238 cm³/s.

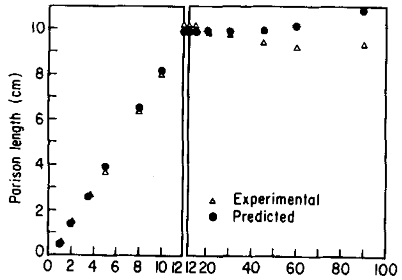

Figure 8. Comparison of experimental and predicted values of parison length. Straight die, m = 9 g, Q = 0.950 cm³/s.

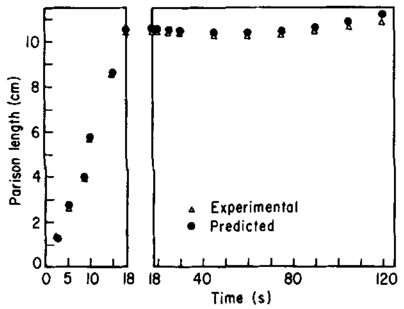

Figure 9. Comparison of experimental and predicted values of parison length. Diverging die, m = 6.8 g, Q = 0.475 cm³/s.

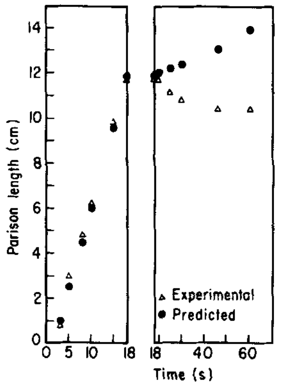

Figure 10. Comparison of experimental and predicted values of parison length. 20° converging die, m = 6.8 g, Q = 0.475 cm³/s.

and data are found to be in good agreement in the extrusion stage and at shorter times in the post-extrusion stage. At longer times the predictions are higher than the experimental data.

For the 20° converging die, it was observed that the model predictions are very poor in the post-extrusion stage. This is shown in Figure 10. The failure of the model for the 20° converging die is thought to be due to the very large diameter swell that occurs with this die. This has the effect of rendering invalid the assumptions that swell and sag are independent phenomena and that sag is equivalent to uniaxial extension. To improve the predictions, sag and swell would have to be modeled as coupled phenomena. This requires a detailed finite element analysis of the process, as the simple, lumped-parameter model described here is no longer valid.

ACKNOWLEDGMENT

This work was supported by grants from the Natural Sciences and Engineering Research Council of Canada and the Quebec Department of Education. The resin was supplied by Union Carbide Canada Ltd.

NOTATION

A_d = cross-sectional area of the die at the exit
A_i = cross-sectional area of the ith element
A_i' = cross-sectional area of the unswollen element
B_1 = diameter swell
B_2 = thickness swell
B_o = instantaneous diameter swell
B_∞ = equilibrium diameter swell
G_{ok} = kth equilibrium relaxation modulus
i = index denoting the parison element
L = length of the parison
L_i = length of the ith element
m = weight of the parison
N = number of parison elements that are fully extruded
Q = volumetric flow rate
t = time
t' = past time
t_c = time lag
t_e = extrusion time
t_i = time elapsed since the ith element was fully extruded
v_d = average melt velocity at the die exit
Z_i = length of the hypothetical unswollen element.

Greek Letters

$\dot{\epsilon}_i$ = extensional strain rate of the ith element
ζ = characteristic time for swell, Eq. 1
$\Delta\theta$ = step size for numerical integration
λ_{ok} = kth equilibrium relaxation time
ρ = density
τ_i = stretching stress of the ith element

LITERATURE CITED

Acierno, D., et al., *J. Non-Newt. Fl. Mech.*, **1**, 125 (1976).
Ajroldi, G., *Polym. Eng. Sci.*, **18**, (10), 742 (1978).
Bird, R. B., R. C. Armstrong, and O. Hassager, *Dynamics of Polymeric Liquids*, 1, 451, John Wiley, New York (1977).
Carnahan, B., H. A. Luther, and J. O. Wilkes, *Applied Numerical Methods*, John Wiley, New York (1969).
Cogswell, F. N., et al., *Plast. Polym.*, **39**, 340 (1971).
Dealy, J. M., and W. Tsang, *J. Appl. Polym. Sci.*, **26**, 1,150 (1981).
Dutta, A., and M. E. Ryan, *J. Non-Newt. Fl. Mech.*, **10**, 235 (1982).
Garcia-Rejon, A., N. Orbey, and J. M. Dealy, *SPE Tech. Papers*, **27**, 431 (1981).
Garcia-Rejon, A., and J. M. Dealy, *Polym. Eng. Sci.*, **22**, 158 (1982).
Henze, E. D., and W. Wu, *Polym. Eng. Sci.*, **13**, 153 (1973).
Kamal, M. R., V. Tan, and D. Kalyon, *Polym. Eng. Sci.*, **21**, 331 (1981).
Lodge, A. S., *Body Tensor Fields in Continuum Mechanics*, 226, Academic Press, New York (1974).
Orbey, N., "Sag and Swell of Extrudate from Annular Dies," Doctoral Dissertation, McGill University, Montreal (1983).
Orbey, N., and J. M. Dealy, *Polym. Eng. Sci.*, **24**, 511 (1984).
Tschoegl, N. W., *Rheol. Acta*, **10**, 582 (1971).
Tschoegl, N. W., *Rheol. Acta*, **12**, 82 (1973).

Manuscript received Oct. 5, 1983; revision received: Mar. 1 and accepted May 2, 1984